Available online at www.sciencedirect.com
ScienceDirect
Ceramics International 37 (2011) 2269–2274
CERAMICS INTERNATIONAL
www.elsevier.com/locate/ceramint

Synthesis and sintering behavior of $La_{0.8}Sr_{0.2}CrO_3$ by a glycine nitrate process

Elizabeth Thomas [a], Da Hae Lee [b], Mi Young Yoon [b], Sheryl.H Ehrman [a], Hae Jin Hwang [a,b,*]

[a] Chemical & Biomolecular Engineering, University of Maryland, College Park, MD, USA
[b] Materials Science and Engineering, Inha University, Incheon, Republic of Korea

Received 8 February 2011; received in revised form 11 March 2011; accepted 11 March 2011
Available online 23 March 2011

Abstract

$La_{0.8}Sr_{0.2}CrO_3$ powder was synthesized by a glycine nitrate process from an aqueous solution of lanthanum, strontium, and chromium nitrates, and glycine. The apparent density, size and morphology of the $La_{0.8}Sr_{0.2}CrO_3$ powder depended on the glycine-to-nitrate ratio. However, the pH value of the precursor solution had no significant effect on these properties. It was found that a single-phase perovskite, $La_{0.8}Sr_{0.2}CrO_3$, was synthesized when the dried ash was calcined at 1200 °C for 5 h. A secondary minor phase, $SrCrO_4$, was observed in the powder calcined at temperatures lower than 1100 °C. The presence of the $SrCrO_4$ phase has a significant effect on the sinterability and microstructural evolution of the $La_{0.8}Sr_{0.2}CrO_3$. A relative density higher than 90% could be achieved when the 1000 °C-calcined $La_{0.8}Sr_{0.2}CrO_3$ powder was sintered at 1450 °C.

Keywords: D. Perovskite; Glycine nitrate process (GNP); Solid oxide fuel cells; $LaCrO_3$

1. Introduction

$LaCrO_3$-based perovskite materials have been widely used as a ceramic interconnect for solid oxide fuel cells (SOFCs) due to their high electrical conductivity, high thermal conductivity and good phase stability under a reducing atmosphere and in air [1,2]. However, these materials have poor sinterability in air and typically require about 1700 °C for achieving densities above 95% of the theoretical using normal solid-state sintering techniques. Although calcium-doped $LaCrO_3$ exhibited better sinterability than strontium-doped $LaCrO_3$, the problem of calcium ion diffusion toward the Ni–YSZ anode during the cell fabrication process at a high temperature remains unsolved [3,4].

Recently, A and B site co-doped $LaCrO_3$ has received a great deal of attention as a potential candidate to replace the Ni–YSZ currently used as the anode material of SOFCs [5–7]. In order to create an anode with sufficient porosity and small enough particles to achieve a high surface area and allow fuel to pass through to the electrode, nano-sized particles are needed. There are various methods of synthesizing ceramic powders, such as a solid state reaction and/or the sol–gel, Pechini and glycine nitrate processes. Of these processes, the glycine nitrate process (GNP) is one of the most attractive methods, as it allows homogeneous nano-sized particles to be obtained via a self-ignited combustion process using metal nitrates and glycine. It also has the advantage of being an easy and speedy process. The amine ($–NH_2$) and carboxyl (–COO) groups can make complexes with metal ions, thus preventing the metal nitrates from segregating before the combustion reaction occurs [8–10].

In this study, Sr-doped $LaCrO_3$ nano powder was synthesized by the GNP from lanthanum, strontium and chromium nitrates and glycine. The phase evolution behavior as a function of the calcination temperature and microstructure of the $LaCrO_3$ were investigated in terms of the glycine-to-nitrate ratio and the pH of the precursor solution. The effect of the calcination temperature on the sinterability of the $LaCrO_3$ powder was also examined.

2. Experimental procedure

In this study, the effects of two processing variables were examined: (1) the glycine-to-nitrate molar concentration ratio

* Corresponding author at: Materials Science and Engineering, Inha University, Incheon, Republic of Korea.
E-mail address: hjhwang@inha.ac.kr (H.J. Hwang).

0272-8842/$36.00
doi:10.1016/j.ceramint.2011.03.025

and (2) the pH value of the precursor solution. Glycine acts as a fuel during the combustion reaction, where it is oxidized by nitrate ions that give off nitrogen, water and carbon dioxide gases. The characteristics of the resulting oxide powder, including the particle size, surface area and density, strongly depend on the temperature during the combustion. This can be controlled by adjusting the glycine-to-nitrate ratio. Glycine also acts as a chelating agent for various metal ions. It contains a carboxylic acid group at one end and an amino group at the other end. While in a solution, glycine turns into a zwitter ion and complexes metal ions, which can be of any ionic size.

Lanthanum, strontium and chromium nitrates and glycine were used as the starting materials. The nitrates and glycine were dissolved in distilled water. The pH value of the solution was approximately 3. The molar ratio of lanthanum to strontium was fixed at 0.8:0.2, while different glycine-to-nitrate ratios, in this case 1:1, 1.5:1 and 2:1, were used. The pH of the precursor solution was also varied using nitric acid. After stirring the precursor solution at 80 °C for 2 h, it was then heated to enable the water to evaporate, causing the solution to become dry. Once the combustion reaction started, it was completed in less than 5 min., with the exact time depending on the amount of starting materials used. The obtained ash was calcined in a tube furnace at 500, 1000 and 1200 °C for 5 h. The $La_{0.8}Sr_{0.2}CrO_3$ (LSC) powders were pressed uniaxially into disks in a WC–Co alloy mold (25 mm in diameter), which was followed by cold isostatic pressing (CIP) at 200 MPa using a rubber mold with a stainless steel cylinder placed in the center. After CIP, the pressed pellets were fired at various temperatures (1400, 1450, 1500 and 1550 °C) for 5 h in air.

For characterization of the phase, X-ray diffraction (XRD, RU-200B, Rigaku Co., Ltd., Japan) was performed using Ni-filtered CuKα radiation. The bulk density was determined using the Archimedes method in water. Thermogravimetric analysis (TG) and differential thermal analysis (DTA) were carried out using a TG–DTA instrument (Diamond TG/DTA, Perkin Elmer, USA). The powder morphology and microstructure were observed by field emission scanning electron microscopy (SEM, JSM-5500, JEOL, Japan).

3. Results and discussion

The apparent density of the powders showed little variation at the same glycine-to-nitrate ratio, apart from different pH values. However, a more significant difference was noted as the glycine-to-nitrate ratios increased. An increase in the glycine molar concentration results in a decrease in the apparent density. The tapping density of the obtained powder was 0.8 and 0.7 g/cm^3 for a glycine-to-nitrate ratio of 1:1 and 2:1, respectively. This could be due to the fact that most of the glycine reacts during combustion, creating pores in the heat-treated powder, thus making the sample more porous. This phenomenon is shown in the SEM images presented in Fig. 5.

Fig. 1 shows XRD patterns of the powders calcined at 500 °C for 5 h, as prepared from precursor solutions having different glycine-to-nitrate ratios and the same pH value. The XRD patterns reveal that the powder, which was prepared from

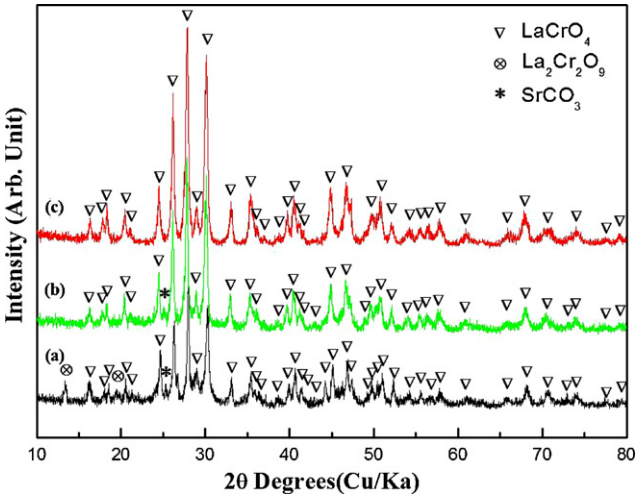

Fig. 1. XRD patterns of samples calcined at 500 °C prepared from precursor solutions with glycine-to-nitrate ratios of 1:1 (a), 1.5:1 (b), and 2:1 (c). The pH value of the solution is 3.

a precursor solution with a glycine-to-nitrate ratio of 1:1, consists of $LaCrO_4$, $La_2Cr_2O_9$, and $SrCO_3$ phases. It is known that $LaCrO_4$ is an intermediate phase before it transforms into a $LaCrO_3$ perovskite when the ash is calcined at a low temperature, as chromium has a tendency to keep its oxidation state high at a low temperature [11,12].

As the glycine molar concentration increases, the XRD patterns become much simpler. Although the $La_2Cr_2O_9$ and $SrCO_3$ phases are still present in the powder at a glycine-to-nitrate ratio of 1.5:1, their peak intensity decreases as the glycine-to-nitrate ratio increases, leading to single-phase $LaCrO_4$ in the powder with a glycine-to-nitrate ratio of 2:1. This observed result indicates that the glycine increases the ability of the cations to create complexes.

The dissociation state of the carboxyl and amino groups of glycine can change depending on the pH value of the precursor solution, which can affect its molecular structure. For example, at pH = 2.34, approximately half of the –COOH groups were ionized, whereas the $–NH_2$ groups were completely ionized [13]. In addition, the amino group and carboxyl group can chelate with the chromium ion and the lanthanum or strontium ion, respectively [9]. Thus, the pH value of the precursor solution can affect the crystallization behavior of the dried ash.

Fig. 2 shows XRD patterns of the powders calcined at 500 °C for 5 h, as prepared from precursor solutions having various pH values and the same glycine-to-nitrate ratio. At pH = 3, the calcined powder is composed mainly of $LaCrO_4$; the minor phase, $SrCO_3$, was also found, as shown in Fig. 1. It appears that the $SrCO_3$ results from the reaction between $Sr(NO_3)_2$ and CO_2 due to the combustion of glycine above at 500 °C. The presence of $SrCO_3$ suggests that the glycine cannot chelate strontium in the precursor solution. On the other hand, the peak intensity of the $SrCrO_3$ phase was greater at pH = 2 than it was at pH = 3 and 1. As the dissociation of the –COOH groups decreased as the pH value decreased, it appears that such a phenomenon is reasonable. However, it is not clear that the peak intensity of the $SrCO_3$ phase becomes smaller again at

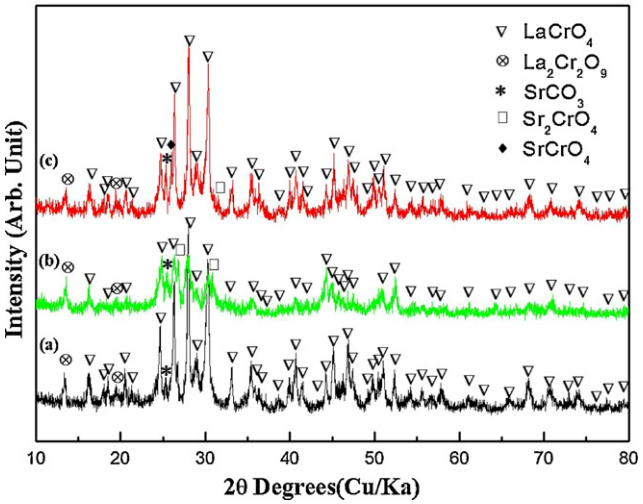

Fig. 2. XRD patterns of samples calcined at 500 °C prepared from the precursor solutions with pH values of 3 (a), 2 (b), and 1 (c). The glycine to nitrate ratio is 1:1.

pH = 1. This tendency was also observed in powder samples prepared from precursor solutions with different glycine-to-nitrate ratios.

A $La_{0.8}Sr_{0.2}CrO_3$ perovskite was formed after calcining the ash above 500 °C; it was prepared from a precursor solution with a pH of 3, the quantity of which increased with an increase in the calcination temperature. Therefore, it can be inferred that the temperature at which the perovskite phase forms decreases as the pH value of the precursor solution increases. In addition, increasing the glycine molar concentration reduces the amount of minor phases of $SrCrO_4$ present, as shown in Fig. 3. The $SrCrO_4$ phase was still noted in all of the powders calcined at 1000 °C. An EDX analysis (Fig. 4) showed that the extant lumps are made up of approximately 48% Sr, 26% Cr and 13% O (mass%). After an XRD examination of these samples, it was considered that this minor phase was $SrCrO_4$. Calcining the ash

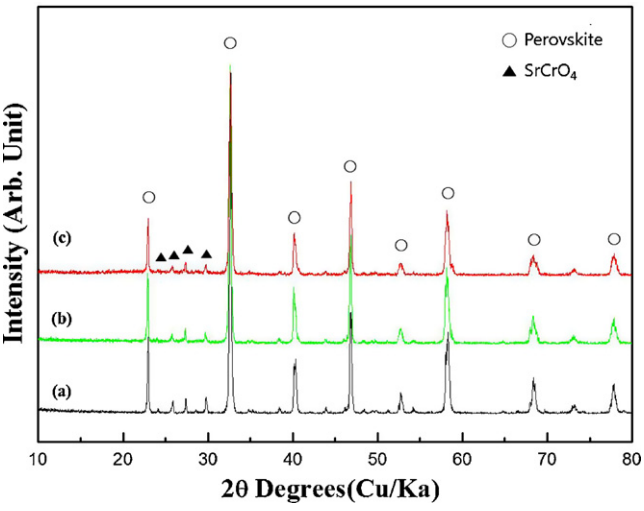

Fig. 3. XRD patterns of samples calcined at 1000 °C prepared from precursor solutions with glycine-to-nitrate ratios of 1:1 (a), 1.5:1 (b), and 2:1 (c). The pH value of the solution is 3.

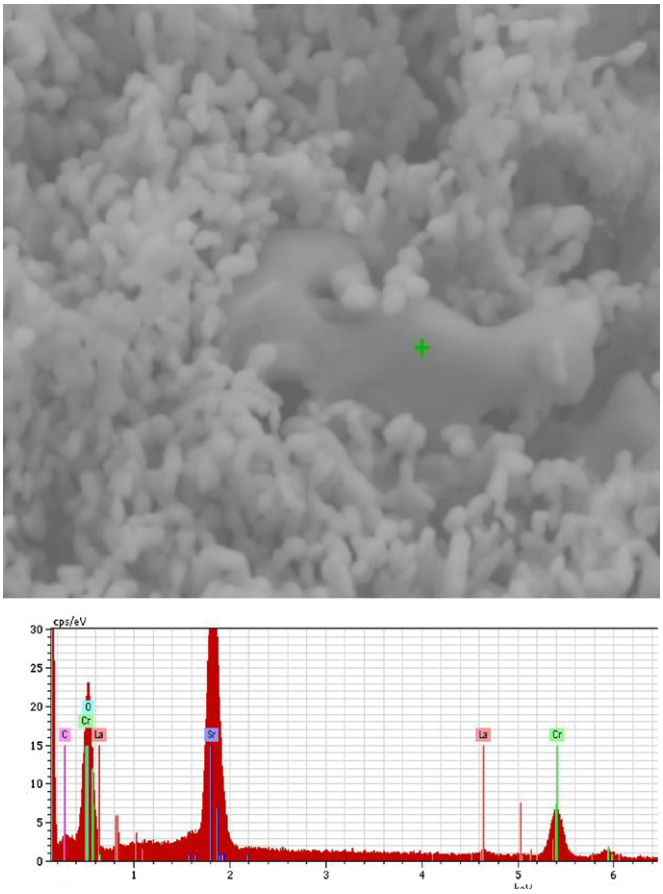

Fig. 4. SEM photograph and EDX analysis of $SrCrO_4$.

at high temperatures in excess of 1200 °C is essential to achieve a single-phase perovskite.

The particle size and apparent density of the powder strongly depend on the glycine-to-nitrate ratio and the calcination temperature. Fig. 5 shows SEM images of powders prepared from precursor solutions having various glycine-to-nitrate ratios. In the SEM images, we observed that an increase in the glycine-to-nitrate ratio led to the production of smaller and more porous particles. Moreover, a reduction in the pH value resulted in smaller particles when the glycine-to-nitrate ratio was 1:1. As the glycine molar concentration increased, it appeared that the pH effect on the particle morphology was slight. The smaller particles were found to have a lower density, as they could agglomerate and thus create clumps, allowing more space in between them and thus reducing the density.

Glycine acts as a fuel during the glycine nitrate process. This process is a rapid self-sustaining process. Thus, increasing the amount of glycine would lead to an increase in the rate of combustion of the metal nitrates and cause the reaction to combust faster and at hotter temperatures, drying out the nitrates and producing smaller primary particles. These particles can aggregate quickly, as they are close together and sticky, leading to the formation of the rod-like structures shown in Fig. 5.

Fig. 6 shows the relative density of the LSC sintered bodies calcined at 1000 and 1200 °C as a function of the temperature. The relative densities of the 1200 °C-calcined LSC samples

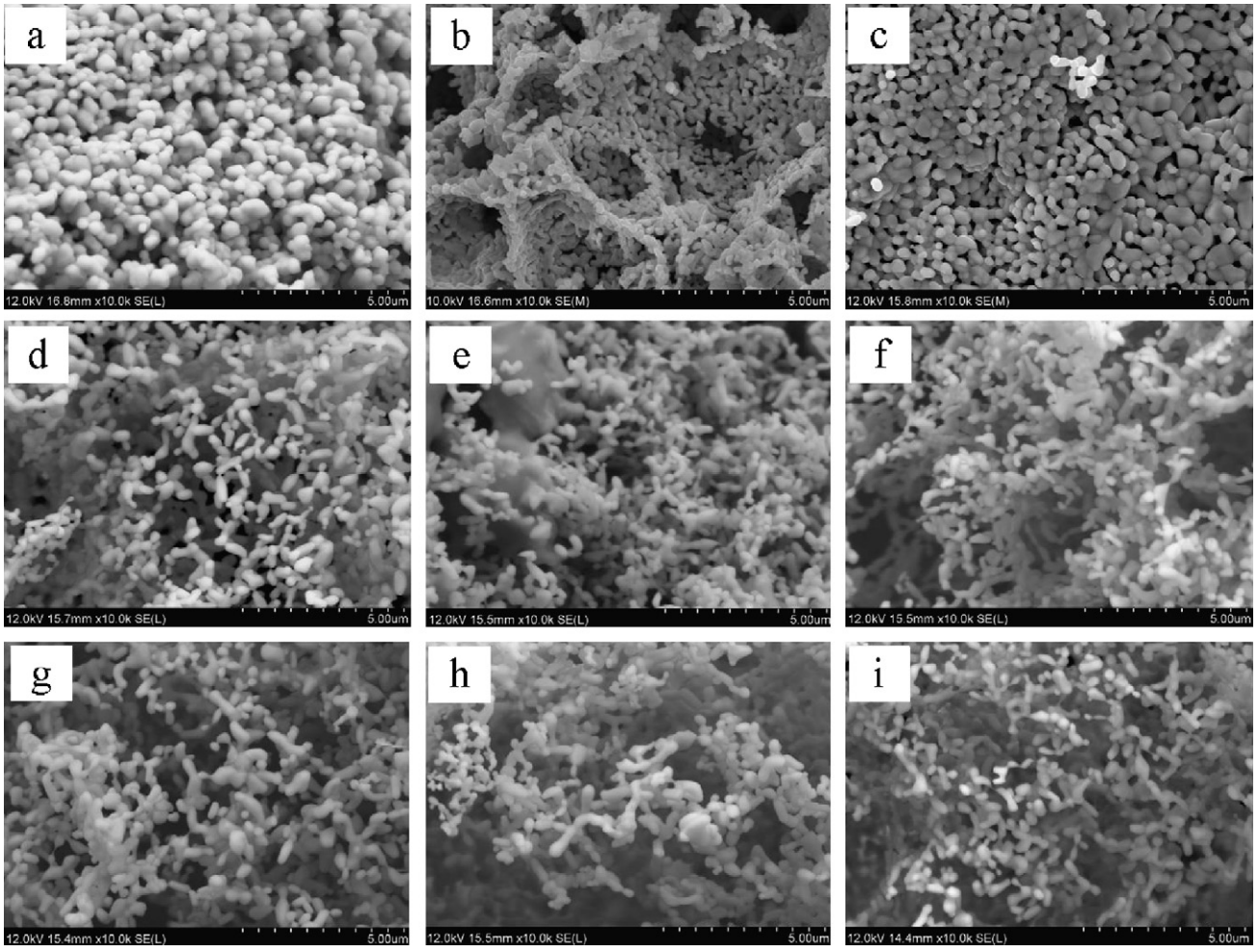

Fig. 5. SEM photographs of La0.8Sr0.2CrO3 powders calcined at 1000 °C with various pH values and glycine-to-nitrate ratios. (a) pH = 3, 1:1 (b) pH = 2, 1:1 (c) pH = 1, 1:1 (d) pH = 3, 1.5:1 (e) pH = 2, 1.5:1 (f) pH = 1, 1.5:1 (g) pH = 3, 2:1 (h) pH = 2, 2:1 (i) pH = 1, 2:1.

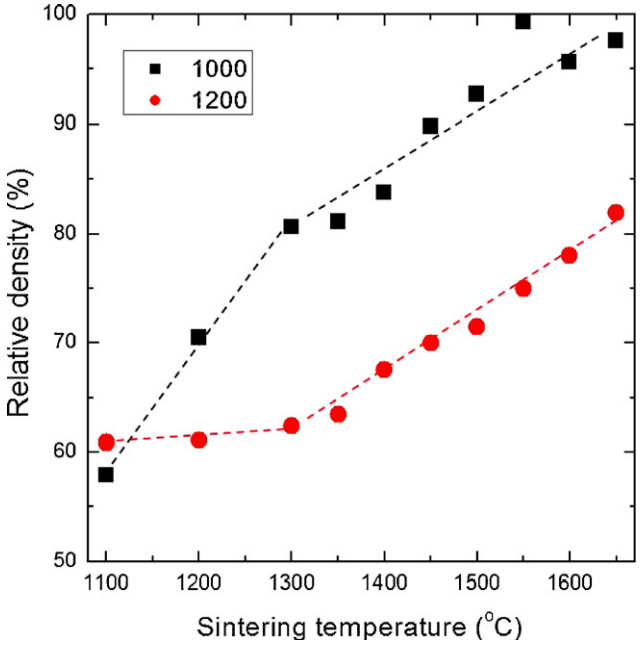

Fig. 6. Relative densities of sintered $La_{0.8}Sr_{0.2}CrO_3$ samples calcined at 1000 °C and 1200 °C as a function of the sintering temperature.

showed a monotonous increase as the sintering temperature increased. An interesting feature shown in Fig. 6 is that the relative densities of the 1000 °C-calcined samples are much higher than those of the 1200 °C-calcined samples. Moreover, the density increases steeply between 1000 °C and 1300 °C. Given that the particle size of the 1000 °C-calcined sample is smaller than that of the 1200 °C-calcined sample, the sintering behavior in Fig. 6 may be reasonable. However, the relative density difference between the two appears to be exceedingly high, which can be expected from the difference in the particle size. This result can be explained by the fact that the $SrCrO_4$ phase can serve as a sintering aid in the intermediate temperature range and can thus be responsible for the good sinterability of the LSC samples. As shown in Fig. 3, the 1000 °C-calcined LSC powder contains $SrCrO_4$ as an impurity phase. In contrast, there is no peak which corresponds to $SrCrO_4$ in the 1200 °C-calcined powder.

The TG–DTA curves of the $SrCrO_4$ and LSC powders calcined at 1000 and 1200 °C are shown in Fig. 7. $SrCrO_4$ exhibited two small endothermic peaks at 1000 °C and 1285 °C. The first peak at 1000 °C is thought to be responsible for the melting of $SrCrO_4$, although some papers have stated that the melting temperature of $SrCrO_4$ is approximate-

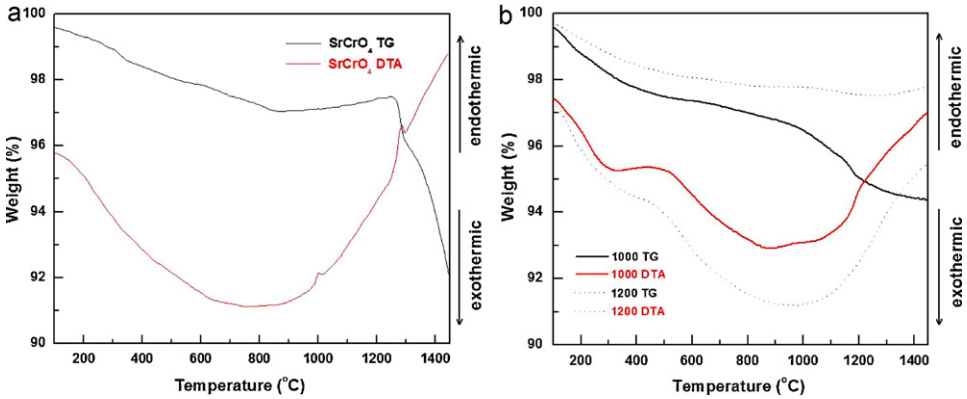

Fig. 7. TG–DTA curves of $SrCrO_4$ (a) and $La_{0.8}Sr_{0.2}CrO_3$ (b) powders. The $La_{0.8}Sr_{0.2}CrO_3$ powder was calcined at 1000 and 1200 °C.

ly1250 °C [14]. The second peak at 1285 °C corresponds to the decomposition of $SrCrO_4$. $SrCrO_4$ is known to decompose to $SrCrO_3$ and oxygen and then dissolve in the $LaCrO_3$ perovskite [15]. The abrupt weight loss at 1285 °C of the TG curve of $SrCrO_4$ suggests that the decomposition occurs at 1285 °C.

On the other hand, no endothermic peak was observed in the DTA curve of the LSC powders calcined at 1000 and 1200 °C. This may be due to the small amount of $SrCrO_4$ included in the LSC powders. However, the 1000 °C-calcined LSC powder shows a TG curve similar to that of $SrCrO_4$; some weight loss occurs at between 1150 and 1350 °C, and this saturates at around 1400 °C. In contrast, there is little weight loss in the TG curve of the 1200 °C-calcined LSC powder. The observed weight loss may be caused by the melting and decomposition of $SrCrO_4$ in the LSC powder. The weight loss between 1150 and 1400 °C was estimated to be 0.516%; assuming that all weight loss is due to the decomposition of $SrCrO_4$; the LSC powder calcined at 1000 °C includes 6.5 wt% of the $SrCrO_4$ phase. It is clear from Fig. 6 that the temperature at which the sintering is accelerated is precisely consistent with the temperature at which the weight loss begins in the TG curve of the 1000 °C-calcined LSC powder. Therefore, the $SrCrO_4$ impurity phase may be associated with the better sinterability observed in the 1000 °C-calcined LSC powder, as described in Fig. 6.

Fig. 8 shows SEM images of the LSC samples sintered at 1450 and 1550 °C. As is evident in Fig. 8(b), the LSC samples calcined at 1200 °C and subsequently sintered at 1450 °C were found to be porous with a grain size of 1–2 μm, suggesting that there was little grain growth at 1450 °C. Even at 1550 °C (Fig. 8(d)), it appears that sintering does not proceed further and

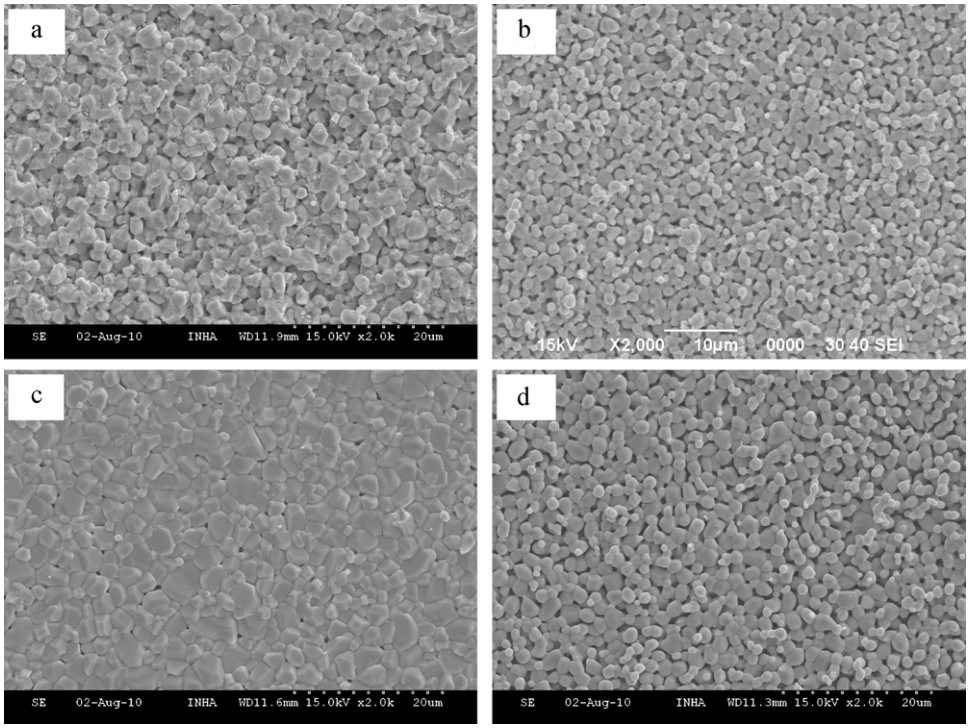

Fig. 8. SEM photographs of the $La_{0.8}Sr_{0.2}CrO_3$ samples sintered at 1450 (a and b) and 1550 °C (c and d). Here, (a), (c), and (b), (d) were samples sintered using the 1000 °C- and 1200 °C-calcined powders, respectively.

that the grain growth is modest. On the other hand, the sintering was significantly enhanced in the LSC sample calcined at 1000, and fully densified LSC can be obtained by sintering the LSC powder at 1550 °C. The grain size of the 1000 °C-calcined LSC is larger than that of the 1200 °C-calcined LSC, which means that the liquid phase sintering mechanism may be incorporated in LSC when it has a small amount of $SrCrO_4$ phase. The electrical conductivities of the LSC samples sintered at 1600 °C were 42 and 33 S/cm at 800 °C in air for the 1000 °C-calcined and 1200 °C-calcined samples, respectively. This means that the $SrCrO_4$ helps the densification, but does not affect the electrical conductivity.

4. Conclusion

$La_{0.8}Sr_{0.2}CrO_3$ powder was synthesized using the glycine nitrate process (GNP) and the resultant combustion ash was calcined at 500 °C, 1000 °C and 1200 °C. The X-ray diffraction results indicated the presence of a minor phase, i.e., $SrCrO_4$, in the samples heat-treated at temperatures below 1100 °C. Additionally, the amount of minor phase present decreases as the glycine concentration is increased.

The glycine affected the morphology of the $La_{0.8}Sr_{0.2}CrO_3$ particles. The addition of glycine likely led to more porous and loosely packed $La_{0.8}Sr_{0.2}CrO_3$ aggregates due to the resulting increase in the combustion rate and the rod-like aggregation of the particles. The pH value of the precursor solution influences the morphology and microstructure of the resultant powder. Reducing the pH value of the samples led to the production of smaller particles and their aggregation.

The LSC powder calcined at 1000 °C showed better sinterability compared to that at 1200 °C, suggesting that the liquid phase due to the $SrCrO_4$ phase accelerated the sintering and grain growth of the LSC powder. A relatively high relative density (above 90%) could be obtained when the 1000 °C-calcined LSC powder was sintered at 1450 °C.

Acknowledgement

This study was supported by the Korea Institute of Energy Research (KIER). Part of this work was supported by the National Research Foundation of Korea (NRF) grant funded by the Korea government (MEST) (No. 2010-0010744)

References

[1] S. Miyoshi, S. Onuma, A. Kaimai, H. Matsumoto, K. Yashiro, T. Kawada, J. Mizusaki, H. Yokokawa, Chemical stability of $La_{1-x}Sr_xCrO_3$ in oxidizing atmospheres, J. Solid State Chem. 177 (2004) 4112–4118.
[2] X. Zhu, H. Gu, H. Chen, Y. Zheng, L. Guo, Effect of Ca^{2+} and Zn^{2+} cations substitution on the properties of $La_{0.85}Sr_{0.15}CrO_3$ as SOFC interconnect, J. Alloys Compd. 480 (2009) 958–961.
[3] J.-H. Kim, D.-H. Peck, R.H. Song, G.-Y. Lee, D.-R. Shin, S.-H. Hyun, J. Wackerl, K. Hilper, Synthesis and sintering properties of $(La_{0.8}Ca_{0.2-x}Sr_x)CrO_3$ perovskite materials for SOFC interconnect, J. Electroceram. 17 (2006) 729–733.
[4] J. Sfeir, $LaCrO_3$-based anodes: stability considerations, J. Power Sources 118 (2003) 276–285.
[5] S.W. Tao, J.T.S. Irvine, J.A. Kilner, An efficient solid oxide fuel cell based upon single-phase perovskites, Adv. Mater. 17 (2005) 1734–1737.
[6] X.J. Chen, Q.L. Liu, S.H. Chan, N.P. Brandon, K.A. Khor, High performance cathode-supported SOFC with perovskite anode operating in weakly humidified hydrogen and methane, Electrochem. Commun. 9 (2007) 767–772.
[7] A.L. Sauvet, J.T.S. Irvine, Catalytic activity for steam methane reforming and physical characterisation of $La_{1-x}Sr_xCr_{1-y}Ni_yO_{3-\delta}$, Solid State Ionics 167 (2004) 1–8.
[8] Y. Ji, J. Liu, T. He, L. Cong, J. Wang, W. Su, Single intermedium-temperature SOFC prepared by glycine–nitrate process, J. Alloys Compd. 353 (2003) 257–262.
[9] Y. Yang, T. Wen, H. Tu, D. Wang, J. Yang, Characteristics of lanthanum strontium chromite prepared by glycine nitrate process, Solid State Ionics 135 (2000) 475–479.
[10] L.A. Chick, L.R. Pederson, G.D. Maupin, J.L. Bates, L.E. Thomas, G.J. Exarhos, Glycine–nitrate combustion synthesis of oxide ceramic powders, Mater. Lett. 10 (1990) 6–12.
[11] A.K. Tyagi, P.K. Sinha, B.P. Sharma, Role of glycine-to-nitrate ratio in influencing the powder characteristics of $La(Ca)CrO_3$, Mater. Res. Bull. 43 (2008) 1573–1582.
[12] J.D. Carter, H.U. Anderson, M.G. Shumsky, Structure and phase transformation of lanthanum chromate, J. Mater. Sci. 31 (1996) 551–557.
[13] T. Peng, X. Liu, K. Dai, J. Xiao, H. Song, Effect of acidity on the glycine–nitrate combustion synthesis of nanocrystalline alumina powder, Mater. Res. Bull. 41 (2006) 1638–1645.
[14] S. Simner, J. Hardy, J. Stevenson, T. Armstrong, Sintering mechanisms in strontium doped lanthanum chromite, J. Mater. Sci. 34 (1999) 5721–5732.
[15] M. Mori, Y. Hiei, N.M. Sammes, Sintering behavior of Ca- or Sr-doped $LaCrO_3$ perovskites including second phase of $AECrO_4$ (AE = Sr, Ca) in air, Solid State Ionics 135 (2000) 743–748.